Journal of Engineering Research

Volume 6 | Issue 3 Article 26

2022

Analytical Study of Creeping Flow through Porous Media Using Stress-Jump Condition

Marwa Elbehairy

Vol. 6 – No. 3, 2022 Journal of Engineering Research (ERJ)

Analytical Study of Creeping Flow through Porous Media Using Stress-Jump Condition

Marwa Elbehairy[1,*], Yasser Gamiel[2], S.T. Assar[2], M. Kamel El Sayed[2]

[1,*] Basic Science Department, Kafrelsheikh Higher Institute of Engineering and Technology, Kafrelsheikh 33511, Egypt.
email: marwa_52549_pg@f-eng.tanta.edu.eg, dr.mkamel123@gmail.com
[2] Department of Physics and Engineering Mathematics, Faculty of Engineering, Tanta University, Tanta 31733, Egypt
email: y_egcglass@f-eng.tanta.edu.eg, s_talaat@f-eng.tanta.edu.eg

***Abstract*- This work investigates the creeping flow problem via a swarm of porous circular cylindrical particles using the cell model technique. Brinkman equation inside the porous cylindrical region is used, and Stokes equation for the clear fluid would be satisfied. The stress-jump condition, together with the continuity of the velocity components and the continuity of normal stress, are employed at the porous-liquid interfaces. In contrast, no-couple stress condition and no-spin condition are used on the outer boundary of the cell. In addition, we are applying no-slip boundary conditions on the surface of the solid core. Our problem is solved analytically, and stream function expressions are derived for the inside and outside flow fields. The influence of the drag force on each porous cylindrical particle in the cell is calculated. The graph depicts the variation of hydrodynamic permeability with various parameters and especially the impact of the jump coefficient. The results of this model may be used to examine the membrane filtration process.**

Keywords: Cylindrical porous Particle-in-cell model - Stokes flow - Brinkman equation – Permeability - Drag force.

I. INTRODUCTION

The fluid flow problem in concentrated media is essential for chemical and industrial applications. A wide range of these applications includes flows through sand beds and oil collectors, sedimentation, and membrane filtration. Membranes are distinguished by a complicated porous structure that can be represented using various models, including curvilinear and rectilinear conduits or assemblages of porous or impermeable cylindrical (spherical) particles. It is well known that the flow inside and outside porous media is governed by Stokes or Brinkman equations and continuity equations. Solving a boundary value problem for these equations is extremely complicated, where porous structures have complex boundaries as known. Many approaches simplify the liquid flow process through porous layers, such as the collocation method, the effective medium approximation, and the cell method.

The Happel-Brenner cell model approach is the most significant in which an outer envelope surrounds each particle as a single unit cell to avoid cumbersome calculations resulting from considering the flow over the entire swarm of particles. Thus, the reduced boundary problem is solved separately for each single unit cell, considering the effects of neighbours particles using appropriate boundary conditions on the outer cell. On the outer hypothetical envelope cell, various boundary conditions correspond to all known models: Happel [1], Kuwabara [2], Kvashnin [3] and Cunningham [4] are applied. Happel [1,5] and Kuwabara [2] assumed cell models with spherical (cylindrical) shapes for both particle and outer envelope. With this formulation, the flow can be axially symmetric and have an analytical solution. The Happel model would vanish on the outer cell boundary, but the vorticity no longer exists there, as expected by the Kuwabara model. Although both formulations produce almost identical velocity fields and drag forces, the Happel formulation does not need an exchange of mechanical energy between the cell and its surroundings.

On the contrary, the Kuwabara formulation requires a small mechanical energy exchange with the surroundings. The viscous dissipation in the fluid layer does not entirely consume the mechanical energy that the sphere provides to the fluid. Instead, a little part is released into the environment. Kvashnin [3], Cunningham [4], and Mehta [6] considered different boundary conditions on the outer surface of the cell using two distinct cell models. Kvashnin [3] assumed that the tangential component of velocity approaches a minimum concerning radial distance at the cell surface, indicating cell symmetry. The tangential velocity has been assumed to be a component of the average fluid velocity by Cunningham [4] and Mehta [6], denoting the homogeneity of the flow on the cell boundary. The particle-in-cell models mentioned above have analytical solutions that are always effectively valuable to several industrial problems. But, in complicated geometry cases, creeping flow solutions for these models have not been determined. Following the approach of Happel and Kuwabara, many authors studied the analytical solutions for simple geometries like cylinders and spheres. Further, particle-in-cell models with particles enclosed with a porous layer have received much attention in the literature.

The drag force produced by porous cylinders inside a viscous fluid at a low Reynolds number has been observed by Stechkina [7]. Depending on the Brinkman model, Pop and Cheng [8] discussed the mathematical formulation of the steady incompressible flow via a circular cylinder submerged in a medium with constant porosity and the exact solution of governing equations. They demonstrated that the tangential velocity increases from zero near the wall to a maximum value at a small distance and then drops to its asymptotic value away from the wall. In addition, the flow separation hadn't occurred at the cylinder's surface, as proved. Depending on Darcy's law for describing the flow in the porous structure, a uniform flow via a permeable heterogeneous circular cylinder was investigated by Singh and Gupta [9].

Furthermore, Gupta [10] discussed the steady creeping flow through a porous cylinder by applying a matched asymptotic technique, as Kaplun [11] had done for an impermeable circular cylinder. Deo [12] applied Happel and Kuwabara boundary conditions when studying stokes flow through a swarm of porous circular cylinders. Lately, Kim and

Yuan [13] studied an effective model for membrane filtration technique to compute its particular resistance to aggregated colloidal cake layers. Using Kuwabara's boundary condition, Deo [14] analyzed the Stokes flow problem across an array of porous circular cylinders-in-cell surrounding an impermeable core. Vasin [15] described another model consisting of an assembly of impervious cylindrical particles enveloped in a porous layer and then evaluated its permeability. Based on the four different boundary conditions on the cell surface, they considered cylinders' transverse, longitudinal, and random orientations relative to fluid flow.

The requirements for solving the governing equations in the porous and fluid regions involve defining the appropriate porous-interface conditions. Due to the non-local form of the volume-averaged strategy, Ochoa-Tapia and Whitaker [16] inferred that the stress jump condition exists at the interface to combine Darcy's law with Brinkman's equation when the matching process needs a discontinuity in stress. Additional stress jump condition involving inertial impacts was developed by Ochoa-Tapia and Whitaker [17] using the Forchheimer equation with the Brinkman correction and the Navier-Stokes equations. In this case, there are two coefficients: one related to extra viscous stress and the other to inertial stress. Because of these interesting applications, numerous papers [18-22] are devoted to this topic. Kuznetsov [23] discussed the flow in conduits partially filled with porous material using the stress-jump boundary condition at the porous-clear fluid interface. Raja Sekhar and Sano [24], who discussed two-dimensional viscous flow via a distorted void inside the porous region, also employed these boundary conditions reasonably recently. As a result, the stress-jump boundary condition fluid-porous interface can not be neglected. Therefore, there is necessary to investigate such issues; hence this work is concerned with studying the slow viscous flow problem of an incompressible Newtonian fluid through an aggregation of concentric clusters of porous particles with cylinder shapes using stress jump condition.

Furthermore, the essence of a stress jump condition consideration affects the formation of porous layers on the surface of rigid particles that result from the dissolution and adsorption of polymers, so a porous layer on the surface of an impermeable cylindrical core is taken into consideration. Any modification in the frictional force on the interface between fluid and solid surfaces, like the colloid particles' surfaces or variation in the overall permeability of the membrane, is due to the formation of porous layers on the surfaces of rigid particles. The Brinkman equation is satisfied to describe the flow in the porous cylindrical shell, whereas the Stokes equation outside these porous regions is used. Applied boundary conditions include the continuity for velocity components, as well as for normal stresses at the porous cylindrical shell and the absence of velocity components on the solid core surface. Uniform velocity and absence of tangential stresses (Happel model) are applied on the hypothetical cell surface. Representative results are compared and presented in both cases using Mathematica software. It has been graphically explained how various factors affect hydrodynamic permeability, and some significantly limiting cases have been discussed.

II. PROBLEM DESCRIPTION AND MATHEMATICAL FORMULATION

A primary assumption used in this investigation is that a periodic mesh of identical coaxial cylindrical particles consists of a solid cylindrical core of radius ***a*** and is enveloped by a porous cylindrical layer having a radius ***b*** and permeability *K*. Meanwhile; we consider a liquid concentric hypothetical cylinder surrounding the porous cylindrical layer and the flow of a viscous Newtonian fluid at small Reynolds numbers (creeping flow) is steady and axisymmetric. Let us suppose that the fluid with uniform velocity ***U*** moves perpendicular to the *z*-axis of three coaxial cylinders from left to right. The radius of this hypothetical cell ***c(c > b)*** is specified so that the volume fraction of the partially porous particles to the volume of a cell equals the volume fraction of particles in the concentrated system, as shown in Fig. 1

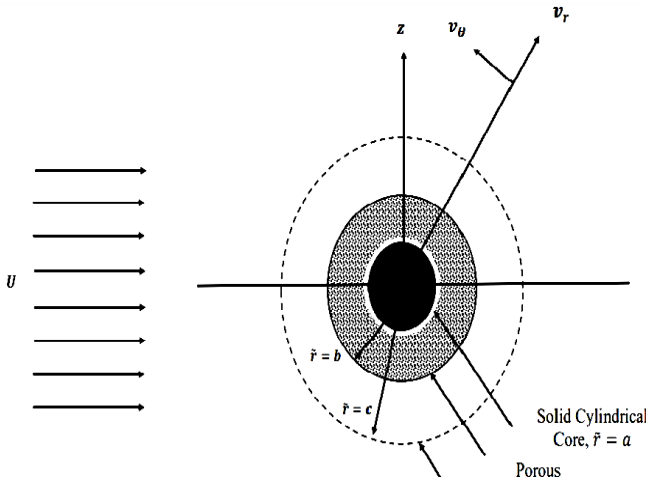

Figure 1. Schematic representation of the physical model and the coordinate system.

Where ε means the porosity, the Stokes and continuity equations are used for an incompressible Newtonian flow with small values for the Reynolds number (creeping flow) outside the porous region ($b \le r \le c$).

$$\left\{\begin{matrix}\tilde{\mu}_1 \nabla^2 \tilde{\mathbf{V}}^{(1)} = \nabla \tilde{P}^{(1)}, \\ \nabla \cdot \tilde{\mathbf{V}}^{(1)} = 0.\end{matrix}\right\} \quad (1)$$

The Brinkman and continuity equations are assumed to govern the flow in the porous cylindrical shell ($a \le r \le b$).

$$\left\{\begin{matrix}\tilde{\mu}_2 \nabla^2 \tilde{\mathbf{V}}^{(2)} - \frac{\tilde{\mu}_2}{\tilde{\mu}_2} \chi^2 \tilde{\mathbf{V}}^{(2)} = \nabla \tilde{P}^{(2)}, \\ \nabla \cdot \tilde{\mathbf{V}}^{(2)} = 0.\end{matrix}\right\} \quad (2)$$

Here, the velocity vector and pressure outside and within the porous cylindrical shell, respectively, are represented by $\tilde{\mathbf{V}}^i, \tilde{P}^i, i = 1,2$ Where $\tilde{\mu}_1$, $\tilde{\mu}_2$ the viscosity coefficients of the liquid are supposed to be constant and equal to improve the correlation between theoretical values and experimental data when determining permeability, the relationship between the dimensionless permeability coefficient $\chi^2 = b^2/k$ and the permeability of the porous layer is inverse.

The cylindrical coordinate system is introduced with z axis directed along the cylinder and a polar axis orientated along the free stream approaching the considered system. The continuity equation for two-dimensional, steady incompressible flow is automatically satisfied when substituting the velocity components (v_r, v_θ) in terms of stream function in polar coordinates form, we get:

$$\frac{\partial v_r^{(i)}}{\partial r} + \frac{v_r^{(i)}}{r} + \frac{1}{r}\frac{v_\theta^{(i)}}{\theta} = 0 \tag{3}$$

$$v_r^{(i)} = \frac{1}{r}\frac{\partial \psi^{(i)}}{\partial \theta}, \qquad v_\theta^{(i)} = -\frac{\partial \psi^{(i)}}{\partial r} \tag{4}$$

Let us proceed to the dimensionless variables and add the following notations for ease of problem analysis: $r = \frac{\tilde{r}}{b}, \boldsymbol{V} = , P = \frac{\tilde{P}}{P_0}, P_o = \mu\frac{U}{b}$. We can get the sets of constitutive equations in the dimensionless form after eliminating the pressure vector in both Eqns. (1) and (2) and using the velocity components (v_r, v_θ) as mentioned above.

$$\nabla^4\psi^{(1)} = 0, \qquad 1 \le r \le \frac{1}{\sqrt{\gamma}} \tag{5}$$

$$\nabla^2(\nabla^2 - \chi^2)\psi^{(2)} = 0, \qquad \lambda \le r \le 1 \tag{6}$$

Also, the tangential and normal stress expressions can be obtained as well as the pressure from the following relations, respectively, as

$$\mathrm{T}_{r\theta}^i = \mu\left(\frac{1}{r}\frac{\partial v_r^i}{\partial \theta} - \frac{v_\theta^i}{r} + \frac{\partial v_\theta^i}{\partial r}\right) \tag{7}$$

$$\mathrm{T}_{rr}^i = -P^i + 2\mu\frac{\partial v_r^i}{\partial r} \tag{8}$$

$$\frac{\partial p^i}{\partial r} = \nabla^2 v_r^i - \frac{v_r^i}{r^2} - \frac{2}{r^2}\frac{\partial v_\theta^i}{\partial \theta} - \chi_i^2 v_r^i \tag{9}$$

III. The Solution to the Problem

The solution of the fourth-order partial differential equations (5) and (6) is obtained by the separation of variables method and can be presented in the form of stream functions in cylindrical coordinates. Suitable stream functions for each region can be given as respectively

$$\psi^{(1)}(r,\theta) = (A\,r + B\,r^3 + \frac{C}{r} + D\,r\ln(r))\sin(\theta) \qquad 1 \le r \le \frac{1}{\sqrt{\gamma}} \tag{10}$$

$$\psi^{(2)}(r,\theta) = (\acute{A}\,r + \acute{B}\,r^3 + \acute{C}I_1(\chi r) + \acute{D}\,K_1(\chi r)\sin(\theta) \qquad \lambda \le r \le 1 \tag{11}$$

where $I_1(\chi r)$and $K_1(\chi r)$are the first-order modified Bessel functions of the first and second kinds, respectively. In our model, we use physically realistic boundary conditions to analyze the flow for each region as follows:

- No-slip condition on the solid core surface $r = \lambda$

$$v_r^{(2)}(\lambda,\theta) = 0, \quad v_\theta^{(2)}(\lambda,\theta) = 0 \tag{12}$$

- Velocity and stress tensor are thought to have continuous normal components on the porous surface $r = 1$, while stress-jump conditions for the tangential components:

$$v_r^{(1)}(1,\theta) = v_r^{(2)}(\lambda,\theta), \; v_\theta^{(1)}(\lambda,\theta) = v_\theta^{(2)}(\lambda,\theta) \tag{13}$$

$$T_{rr}^{(1)}(1,\theta) = T_{rr}^{(2)}(\lambda,\theta) \tag{14}$$

$$\frac{\partial v_\theta^{(2)}(1,\theta)}{\partial r} - \frac{\partial v_\theta^{(1)}(1,\theta)}{\partial r} = \eta\lambda\, v_\theta^{(2)} \tag{15}$$

- No shear stress (Happel condition) on the surface of the hypothetical cell $r = 1/\sqrt{\gamma}$ to mimic the existence of other aggregates of the same size in the vicinity:

$$T_{r\theta}^{(1)}\left(\frac{1}{\sqrt{\gamma}},\theta\right) = 0 \tag{16}$$

- The radial component of velocity on the outside cell surface is continuous as follows:

$$v_r^{(1)}\left(\frac{1}{\sqrt{\gamma}},\theta\right) = U\cos(\theta) \tag{17}$$

We are using the boundary conditions from Eqns. (12) - (17), we can calculate the values of the eight arbitrary constants shown in the Appendix for reader convenience.

IV. Evaluation of Drag Force and Hydrodynamic Permeability

An essential aspect of the flow problem we are studying is drag force. Therefore, the impact of the stress jump values on the drag force and hydrodynamic permeability is the most significant result of our investigation. The force applied to the cylinder during the flowing fluid is known as drag. It is assessed by adding the normal and tangential stress components' contributions to the force acting along the flow direction.

$$F = \int_0^{2\pi}(T_{rr}|_{r=1}\cos(\theta) - T_{r\theta}|_{r=1}\sin(\theta))\,d\theta \tag{18}$$

Therefore, we can get the normal and tangential stress values

$$T_{rr}^{(1)}(r,\theta) = -\frac{4\mu U}{b}\left(Br + \frac{C}{r^3} - \frac{D}{r}\right)\cos(\theta) \tag{19}$$

$$T_{r\theta}^{(1)}(r,\theta) = -\frac{4\mu U}{b}\left(Br + \frac{C}{r^3}\right)\sin(\theta). \tag{20}$$

Substituting Eqns (19) and (20) into Eqn. (18) and integration, one obtains

$$F = 4\mu\pi UD. \tag{21}$$

The hydrodynamic permeability of a membrane which is a significant physical characteristic, can be defined as the ratio of the uniform flow rate to the cell gradient pressure:

$$\overline{L_{11}} = \frac{U}{F / \bar{\bar{V}}} \tag{22}$$

where $\bar{V} = \pi c^2$ the volume of the unit length cell. We can get the hydrodynamic permeability of the system by substituting the drag force value from Eq. (21) into Eq. (22).

$$\overline{L_{11}} = \frac{b^2}{4\mu\gamma D} = L_{11}\frac{b^2}{\mu} \tag{23}$$

$L_{11} = 1/4\gamma D$ is the non-dimensional form of hydrodynamic permeability, which is dependent on three parameters (γ, λ, χ).

Fig. 2 illustrates that the hydrodynamic permeability decreases with increasing χ. This response is quite natural due to the concept of χ. It is inversely proportional to the square root of the permeability of the porous media, which indicates the properties of filtration flow. Meanwhile, an increase in stress jump coefficient η, which describes the role of the tangent stress jump at the interface, enhances the hydrodynamic permeability profile compared with Deo [14] at $\lambda = 0.5, \gamma = 1$. Deo [14] has reported that a decrease in dimensionless hydrodynamic permeability results from an increase in the permeability parameter value. Here, we observed that a stress jump coefficient $\eta = 0.7$ has the most significant effect on the permeability at a particular value $\chi \to 2$. This result reports the improvement of hydrodynamic permeability for a viscous fluid flow that moves perpendicular to a system composed of a solid cylinder covered with a porous layer. The dotted line in Fig. 2 shows higher values of L_{11} up to a certain value when at $\lambda = 0.5, \gamma = 0.8,\ \eta = 0.7$ and χ approaches to 2.4.

Fig. 3 presents the hydrodynamic permeability behaviour in logarithmic coordinates and compares our results with the data reported in [15], where a membrane is composed of a periodic set of identical impenetrable cylinders covered with a porous layer.

As can be seen from this figure, the solid line nearly coincides with what is obtained by [15] in Fig. 3 when $\lambda = 0.5$ and $\gamma = 0.8$. A more noticeable increase in the natural logarithm of dimensionless hydrodynamic permeability is observed, $\eta = 0.7$, from the solid line. From a physical viewpoint, the permeability and volume fraction variations that cause the velocity of the fluid flowing through the porous media to change are related to the stress jump coefficient, which depends on the features of the porous media. As a result, the physical significance of these jump coefficients might be attributed to the associated enhancements in permeability or porosity. On the other side, small values of the natural logarithm of dimensionless hydrodynamic permeability are obtained by choosing $\eta = 0.7$.

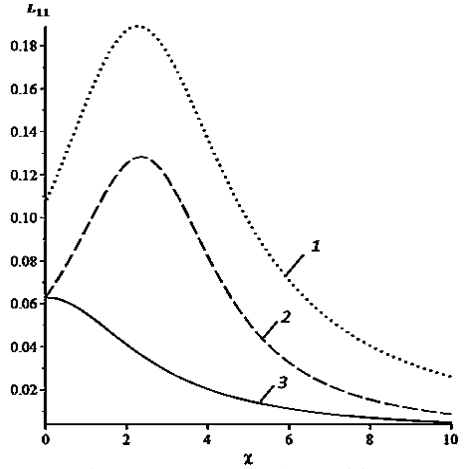

Figure 2. Variation of L_{11} against χ when $\lambda = 0.5$ for solid cylindrical particles covered with a porous layer in a homogeneous fluid flow for different cases: (*1*) $\eta = 0.7, \gamma = 0.8$, (*2*) $\eta = 0.7, \gamma = 1$ and (*3*) Deo [14] $\eta \to 0, \gamma = 1$.

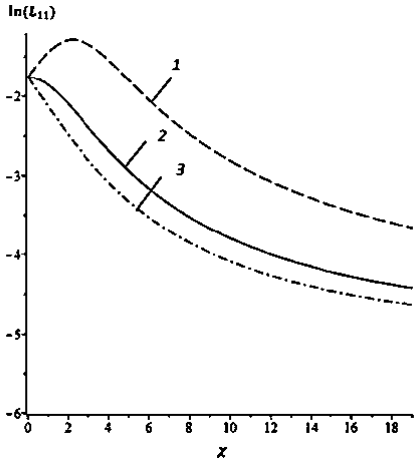

Figure 3. Variation of L_{11} against χ solid cylindrical particles covered with a porous layer in a homogeneous fluid flow when $\lambda = 0.5$ and $\gamma = 0.8$ for different cases: (*1*) $\eta = 0.7$, (*2*) vasin2009 $\eta \to 0$ and (*3*) $\eta = -0.7$.

Fig. 4 shows the pattern of the curves corresponding to a monotonic reduction in the natural logarithm of hydrodynamic permeability to a limiting value at $\gamma \to 1$ for all cases. The natural logarithm of dimensionless hydrodynamic permeability is higher when a more justified stress jump coefficient $\eta = 0.8$ affects fluid flow at the porous-liquid interface. A system of porous circular cylinders, each of radius ***b,*** will be produced when the rigid core vanishes $\lambda \to 0$, i.e. $a \to 0$.

It should be confirmed that the structure of porous circular cylinders has more permeability than an assembly of porous cylindrical particles with a solid core curve (*3)* because more flow can penetrate through the porous media. The negative stress jump coefficient $\eta = -0.8$ influence is less dominant on the natural logarithm of hydrodynamic permeability, as presented in a curve (*4*). In short, we can observe that the natural logarithm of hydrodynamic permeability corresponding to the positive jump coefficient overestimates the other cases.

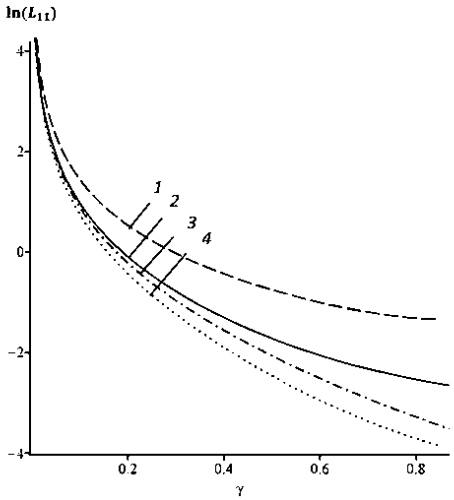

Figure 4. Variation of $\ln(L_{11})$ against χ solid cylindrical particles covered with a porous layer in a homogeneous fluid flow when $\gamma = 0.8$ for different cases: (1) $\eta = 0.8, \lambda = 0.5$ (2) $\eta \to 0, \lambda - .0$, (3) $\eta \to 0, \lambda = 0.5$ and, (4) $\eta = -0.8$, $\lambda = 0.5$

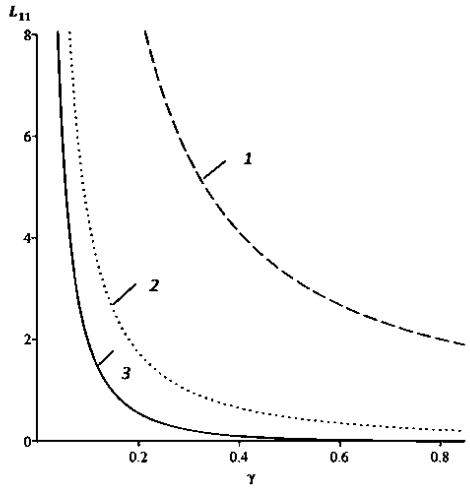

Figure 5. Variation of L_{11} against γ for a system of porous circular cylinders in a homogeneous fluid flow when $\lambda \to 0, \eta = 0.5$ for different cases: (1) $\chi = 1$, (2) $\chi = 3$ and (3) $\chi = 20$.

Fig. 5 exhibits the variation in hydrodynamic permeability with γ and χ for a swarm of porous cylindrical particles of radius b. We noticed that L_{11} decreases with increasing γ since the radius c of the outer cylindrical cell decreases at high values of γ .This causes the particles to approach the walls more closely and experience more drag. In addition, this decrease occurs more rapidly for higher levels o χ. As we stated above, the hydrodynamic permeability reflects distinct and enhanced behavior because of the action of stress jump coefficient $\eta = 0.5$ when comparing this result with the published values in Deo [14].

Fig. 6 shows the same previous behavior but for porous cylindrical particles with an impermeable core under the stress jump condition. Again, a reduction in permeability for porous cylindrical particles with an impermeable core is expected since the exposed solid core causes higher resistance to the imposed flow.

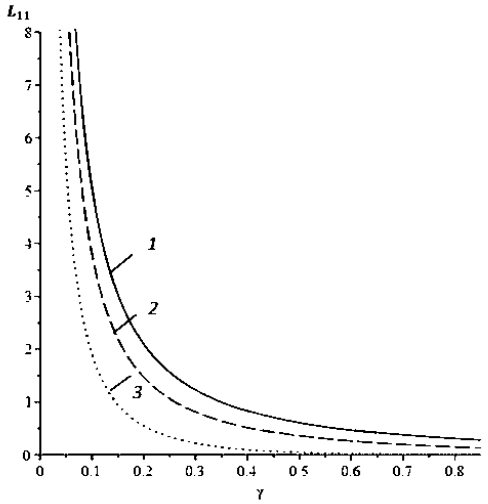

Figure 6. Variation of L_{11} against γ for porous cylindrical particles with an impermeable core when $\lambda = 0.3, \eta = 0.5$ for different cases: (1) $\chi = 1$, (2) $\chi = 3$ and (3) $\chi = 20$.

It can be noticed from Fig. 7 that the trend of hydrodynamic permeability variation with χ is the same as the permeability behavior shown in Deo [14] for a system of porous cylindrical particles inside a homogeneous fluid. The hydrodynamic permeability rapidly decreases for high values of γ. Another observation stands here that the effect of the stress jump coefficient is not seen for a set of porous cylindrical particles

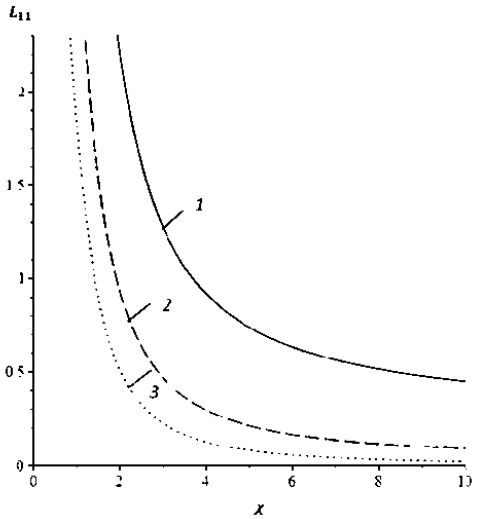

Figure 7. Variation of L_{11} against χ for a system of porous circular cylinders in a homogeneous fluid flow when $\eta = 0.5$, $\lambda \to 0$ for different cases: (1) $\gamma = 0.25$, (2) $\gamma = 0.5$, (3) $\eta \to 0, \lambda = 0.5$ and, (4) $\eta = -0.8$, $\lambda = 0.5$.

V. RESULTS AND DISCUSSION

Using the cell model technique, this study aims to investigate the creeping flow problem through a swarm of porous circular cylindrical particles. Brinkman equation and the Stokes equation are employed inside and outside the porous cylindrical region, respectively. At the porous-liquid interfaces, the stress-jump condition is used along with the continuity of the velocity components and the continuity of

normal stress. on the outer boundary of the cell, no-couple stress and no-spin conditions are applied. Additionally, we are applying no-slip boundary conditions to the surface of the solid core. The dependence of hydrodynamic permeability on stress jump condition is investigated. It can be observed that when the jump coefficient increases, the hydrodynamic permeability reaches a maximum and then begins to decrease. The hydrodynamic permeability increases with jump coefficient signifying lesser flow resistance for a higher shear stress in porous region compared to the clear fluid region. Consequently, stress jump condition caused significant changes in permeability. All the previously stated results have been verified as limiting cases which in good agreement with this study.

Acknowledgement

The authors are grateful to the anonymous reviewers for their encouraging comments and constructive suggestions, which have improved the quality of the manuscript.

Funding: This research received no external funding.

Conflicts of Interest: The authors declare that they have no conflict of interest.

REFERENCES

[1] J. Happel, "Viscous flow in multiparticle systems: Slow motion of fluids relative to beds of spherical particles," *Aiche Journal*, vol. 4, no. 2, pp. 197-201, 1958.

[2] S. Kuwabara, "The forces experienced by randomly distributed parallel circular cylinders or spheres in a viscous flow at small Reynolds numbers," *Journal of the physical society of Japan*, vol. 14, no. 4, pp. 527--532, 1959.

[3] A. Kvashnin, "Cell model of suspension of spherical particles," *Fluid Dynamics*, vol. 14, no. 4, pp. 598--602, 1979.

[4] E. Cunningham, "On the velocity of steady fall of spherical particles through a fluid medium," *Proceedings of the Royal Society of London. Series A, Containing Papers of a Mathematical and Physical Character*, vol. 83, no. 563, pp. 357--365, 1910.

[5] J. Happel, "Viscous flow relative to arrays of cylinders," *AIChE Journal*, vol. 5, no. 2, pp. 174--177, 1959.

[6] G. D. Mehta and T. F. Morse, "Flow through charged membranes," *Journal of Chemical Physics*, vol. 63, no. 5, pp. 1878-1889, 1975.

[7] I. Stechkina, "Drag of porous cylinders in a viscous fluid at low Reynolds numbers," *Fluid Dynamics*, vol. 14, no. 6, pp. 912--915, 1979.

[8] I. a. C. P. Pop, "Flow past a circular cylinder embedded in a porous medium based on the Brinkman model," *International Journal of Engineering Science*, vol. 30, no. 2, pp. 257--262, 1992.

[9] M. a. G. J. Singh, "The flow of a viscous fluid past an inhomogeneous porous cylinder," *ZAMM-Journal of Applied Mathematics and Mechanics/Zeitschrift Angewandte Mathematik und Mechanik*, vol. 51, no. 1, pp. 17--25, 1971.

[10] J. Gupta, "Fluid motion past a porous circular cylinder with an initial pressure gradient," *Journal of Applied Mechanics*, vol. 47, no. 3, p. 489, 1980.

[11] S. Kaplun, "Low Reynolds number flow past a circular cylinder," *Journal of Mathematics and Mechanics*, pp. 595--603, 1957.

[12] S. Deo, "Stokes flow past a swarm of porous circular cylinders with Happel and Kuwabara boundary conditions," *Sadhana*, vol. 29, no. 4, pp. 381--387, 2004.

[13] A. S. a. Y. R. Kim, "A new model for calculating specific resistance of aggregated colloidal cake layers in membrane filtration processes," *Journal of Membrane Science*, vol. 249, no. 1-2, pp. 89--101, 2005.

[14] S. a. Y. P. K. a. T. A. Deo, "Slow viscous flow through a membrane built up from porous cylindrical particles with an impermeable core," *Applied mathematical modelling*, vol. 34, no. 5, pp. 1329--1343, 2010.

[15] S. a. F. A. Vasin, "Cell models for flows in concentrated media composed of rigid impenetrable cylinders covered with a porous layer," *Colloid journal*, vol. 71, no. 2, pp. 141--155, 2009.

[16] J. A. a. W. S. Ochoa-Tapia, "Momentum transfer at the boundary between a porous medium and a homogeneous fluid—I. Theoretical development," *International Journal of Heat and Mass Transfer*, vol. 38, no. 14, pp. 2635--2646, 1995.

[17] J. A. a. W. S. Ochoa-Tapia, "Heat transfer at the boundary between a porous medium and a homogeneous fluid: the one-equation model," *Journal of Porous Media*, vol. 1, p. 1, 1998.

[18] A. a. R. S. G. Bhattacharyya, "Effect of stress jump condition—Viscous flow past a porous sphere with an impermeable core," *Chem. Eng. Sci*, vol. 59, no. 21, pp. 4481--4492, 2004.

[19] A. a. R. S. G. Bhattacharyya, "Stokes flow inside a porous spherical shell: Stress jump boundary condition," *Zeitschrift f"ur angewandte Mathematik und Physik ZAMP*, vol. 56, no. 3, pp. 475--496, 2005.

[20] M. a. M. P. a. R. S. G. Partha, "Viscous flow past a porous spherical shell—effect of stress jump boundary condition," *Journal of engineering mechanics*, vol. 131, no. 12, pp. 1291-1301, 2005.

[21] G. R. a. P. M. a. M. P. Sekhar, "Viscous flow past a spherical void in porous media: effect of stress jump boundary condition," *Journal of Porous Media*, vol. 9, no. 8, 2006.

[22] P. K. a. T. A. a. D. S. a. F. A. a. V. S. Yadav, "Hydrodynamic permeability of membranes built up by spherical particles covered by porous shells: effect of stress jump condition," *Acta Mechanica*, vol. 215, no. 1, pp. 193--209, 2010.

[23] A. Kuznetsov, "Analytical investigation of the fluid flow in the interface region between a porous medium and a clear fluid in channels partially filled with a porous medium," *Applied Scientific Research*, vol. 56, no. 1, pp. 53--67, 1996.

[24] G. a. S. O. Raja Sekhar, "Viscous flow past a circular/spherical void in porous media-an application to measurement of the velocity of groundwater by the single boring method," *Journal of the Physical Society of Japan*, vol. 69, no. 8, pp. 2479--2484, 2000.